Proceedings of the 28th IEEE
EMBS Annual International Conference
New York City, USA, Aug 30-Sept 3, 2006

Automated Removal of Stimulus Artifact in Nerve Conduction Studies

Brian H. Tracey, *Member, IEEE,* and Srivathsan Krishnamachari, *Member, IEEE*

***Abstract*— An algorithm for automated removal of stimulus artifact has been developed and tested on nerve conduction study data. The algorithm uses a hardware-based model of the stimulus artifact (SA). Model parameters are estimated from portions of the data that are judged to contain only the artifact. The model can be used to remove SA even when it is temporally overlapped with the nerve signal. Data are shown to demonstrate the algorithm's performance and to quantify the effect of SA removal on clinical parameters.**

I. Introduction

Nerve conduction studies (NCS) provide a sensitive means for detecting a variety of peripheral nervous system disorders [1 and references therein]. A set of surface electrodes is placed against the skin overlying a nerve and a brief stimulus current applied. If the current is of sufficient magnitude, it triggers a wave of membrane depolarization that spreads bi-directionally outward from the stimulus site. This wave of depolarization, detected with surface electrodes placed overlying the nerve at a site remote from the original stimulus, is referred to as a compound sensory nerve action potential (SNAP). Example SNAP signals are shown in Fig. 1. If this wave of membrane depolarization terminates at a neuromuscular junction (motor endplate zone), the muscle membranes depolarize with resultant muscle contraction. In motor NCS, the muscle evoked response, termed a compound motor action potential (CMAP), is measured and analyzed.

NCS results are interpreted by comparing the patient's response to a normative reference. Prolongation of motor or sensory latencies can indicate nerve compression with injury to the nerve's myelin sheath, as can be seen in carpal tunnel syndrome (median nerve entrapment at the wrist) or ulnar neuropathy at the elbow. The CMAP and SNAP amplitudes are also clinically significant parameters. For example, low sural nerve SNAP amplitude is a sensitive indicator of polyneuropathy in diabetic patients [2]. The accuracy with which response parameters are measured critically influences NCS clinical utility. Unreliable parameters degrade accuracy and may even lead to incorrect diagnoses.

A common problem with NCS is that stimulus artifact (SA) can distort the nerve signal. This is especially true for sensory as compared to motor studies due to the much higher amplifier gains employed with the former. An example is seen in the lower panel of Fig. 1, where SA distorts the apparent SNAP amplitude. While several mechanisms can give rise to SA [3,4], the artifact in Fig. 1 is most likely due to spreading of residual stimulus current through the body tissue. Ideally, stimulus and recording sites would be spatially separated so SA would decay before the nerve signal arrives, but this is not always possible due to anatomical constraints. During traditional non-automated testing, SA can sometimes be minimized by rotating the stimulator anode [5]. Recent work has led to the development of automated NCS using standardized electrode geometries [1]. The fixed electrode geometry has significant advantages in terms of test repeatability and robustness, but requires that SA be reduced by hardware design or signal processing rather than by manual adjustment of stimulating electrode placement.

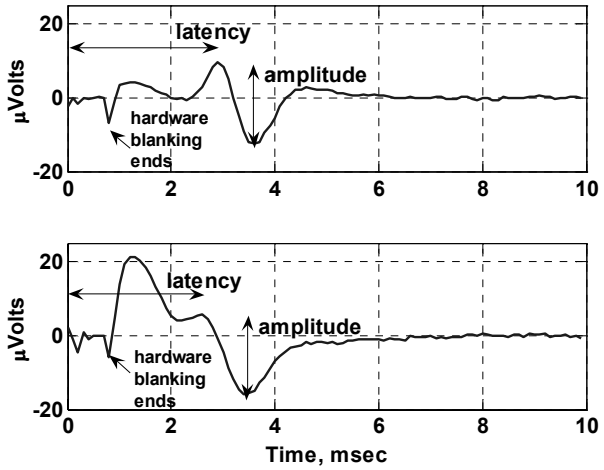

Fig. 1 Example sural nerve NCS. The downward spike at 1 msec is associated with opening of a hardware switch that blanks earlier SA. The rounded waveform peaking between 1-2 msec is the SA; a biphasic SNAP waveform is seen at roughly 3 msec. In the top panel the artifact decays before SNAP onset, while in the bottom panel it significantly overlaps the SNAP.

A variety of methods for reducing SA have been proposed [3-8]. Hardware design can reduce the artifact [3], as further discussed below. One class of signal processing approaches uses auxiliary data to estimate the SA, which is then subtracted from the data. Auxiliary data may include off-nerve recordings or on-nerve recordings using low-level

Manuscript received April 5, 2006. B.H. Tracey is with Neurometrix, Inc., 62 Fourth St, Waltham MA 02451 (phone: 781-314-2753; fax: 781-890-1556; e-mail: brian_tracey@neurometrix.com).

S. Krishnamachari is with Neurometrix, Inc., 62 Fourth St, Waltham MA 02451 (e-mail: srivathsan_krishnamachari@neurometrix.com).

stimuli which includes the SA but not the desired nerve response [3,6]. A difficulty in these approaches is that the SNAP feature may contaminate the auxiliary data. In addition, the SA shape may change with stimulus level or recording location. A second class of signal processing approaches model the stimulus artifact by fitting polynomials, splines, or exponential curves to the data [7,8]. The estimated artifact is subtracted from the data.

In this paper we describe use of a hardware-based model of the SA to estimate and subtract the artifact. This approach differs from previous studies [7,8] in that it utilizes a detailed description of the data acquisition hardware. Model parameters are estimated using data from time periods during which the SNAP is judged to be absent. The model is then used to estimate SA shape during the entire recording. The model is capable of handling SA that was clipped by the data acquisition hardware. If the estimated SA shape passes goodness-of-fit tests, it is used to correct the recorded data. The algorithm was developed for automated NCS testing done with a widely used electrodiagnostic instrument. Data results are shown to demonstrate algorithm performance and to illustrate the impact of SA removal on clinical parameters.

II. DATA ACQUISITION HARDWARE AND MODEL OF STIMULUS ARTIFACT

The NCS data used in this study were acquired with the NC-Stat device (NEUROMetrix, Inc, 62 Fourth St, Waltham MA 02451 USA). Data processing for NC-Stat is done using automated algorithms to extract clinically significant waveform features. The device uses an integrated biosensor with stimulator, detector, and reference electrodes. A constant current stimulator is used.

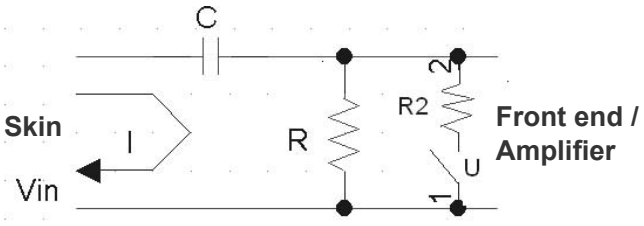

Fig. 2 Circuit diagram showing hardware blanking. The switch U can be closed to effectively blank out the input voltage (note R2<<R). This stage is followed by a second high-pass filter.

Fig. 2 shows a circuit diagram for the first stage of the analog front end. A second high-pass RC filter follows the circuit shown in Fig. 2. During and just after the stimulus, a blanking switch U is closed. This causes current to flow through a low-impedance shunt path, shielding the analog front end from the stimulus. After a fixed time, the blanking switch is opened and the circuit functions as a high-pass filter. The capacitor C can acquire a charge prior to the switch opening. When the switch is opened, the capacitor discharges into the front end. At the same time, residual stimulus currents on the skin are measured by the recording electrodes. These two inputs create the characteristic rising-and-falling shape seen between 1-2 msec in Fig. 1.

A model of the artifact is derived by assuming that the input voltage causing the SA is a decaying exponential with unknown amplitude and decay constant. This assumption is consistent with published results [3,4]. The response of the acquisition system to this input can be calculated. The response of the two high pass filter stages (taking into account the initial charge on the capacitor) is found to be

$$f(t) = A\left(\frac{-k_1}{1-\frac{k_1}{k_2}}\right)\left(\frac{e^{-k_2 t}}{(k_2-k_1)} + \frac{te^{-k_2 t}}{\left(k_1/k_2\right)} - \frac{e^{-k_1 t}}{(k_2-k_1)}\right) \quad (1)$$

where $k_1 = 1/RC$ is the time constant of a single high pass filter, and A and k_2 are the unknown amplitude and time constant of the input exponential. Note from Eq. 1 that the analog front-end transforms the exponential input into a SA which grows initially, then decays at longer times.

III. ALGORITHM DESCRIPTION

The parameters of the artifact model must be estimated from the data on a trace-by-trace basis. The algorithm is as follows:

1. Clipped regions of the waveform are identified and excluded from analysis. If clipped data exists in the latency region where the SNAP is expected, the waveform is discarded.
2. The time of the peak SA is estimated. Based on this time, a look-up table based on Eq. 1 is used to flag samples where the artifact should have significant energy. This provides a first estimate of the region used to fit the artifact model.
3. The approximate onset of the SNAP waveform is estimated using threshold tests on the 1st and 2nd derivatives of the data. The SA fit region is reduced, if necessary, so it ends before the SNAP onset. Thresholds for identifying SNAP onset were determined empirically with the goal of providing a highly sensitive test.
4. A search over possible time constants is carried out. For each k_2, an unscaled SA curve is calculated by using Eq 1 with $A=1$. Amplitude is then estimated as: $A = median(x(\vec{n}) / f(\vec{n} | A = 1))$, where x is the data, $\vec{n}$ is the vector of time samples used for the model fit, and f is the stimulus artifact model. The mean-squared error (MSE) between the data and the SA model in the region $\vec{n}$ is tabulated and used to determine the time constant and amplitude which yield the best fit.

5. Goodness-of-fit tests are used to judge whether an acceptable fit has been achieved. Goodness-of-fit was judged using the normalized error as a metric:

$$\varepsilon = \frac{\frac{1}{N}\sum_n (x[n] - f[n])^2}{\frac{1}{N}\sum_n (x[n])^2} \le 0.03 \qquad (2)$$

where the SA model f includes the amplitude determined in step 4.

6. If the fit is acceptable, a baseline subtracted waveform $x' = x - f$ is used for analysis.

IV. ARTIFACT CORRECTION AND DATA RESULTS

The algorithm was tested on two datasets. First, a reference dataset was created in which the SNAP latency and amplitude are known exactly. This allows algorithm performance to be quantified. A database of sural nerve measurements was mined to find tests in which only SA was seen (no SNAP) and tests in which no artifact was seen (only SNAP). The representative SA and SNAP waveforms were delayed, scaled and added to construct a set of 24 sural tests in which the true SNAP latencies and amplitudes are known. The examples were constructed to be challenging, i.e. SA overlapped the SNAP signal. These tests were processed using an automated SNAP parameter estimation algorithm both with and without SA correction.

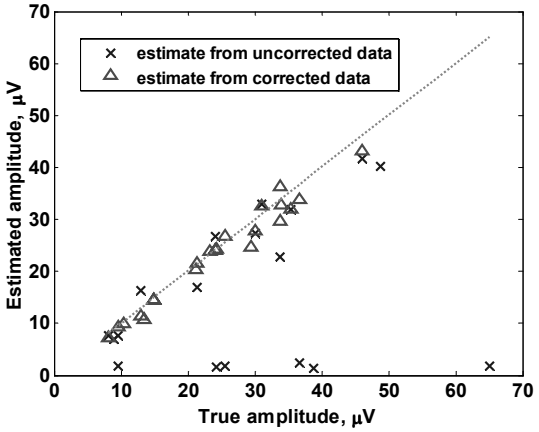

Fig. 3: Scatterplot of amplitude estimates for test dataset with known SNAP parameters.

When the 24 tests were processed without artifact correction, the parameter assignments corresponded to the actual SNAP 11 times, spurious estimates were obtained 5 times, and no estimate was returned 8 times. After removal of the SA, a correct assignment was made 22 of 24 times (no estimate was returned in the other 2 cases). For tests where correct assignments were made, SA removal reduced both the mean and standard deviation of errors in SNAP parameters. Latency errors were reduced from 0.01±0.1 ms to -0.005±0.02 ms (mean ± SD). Amplitude errors were reduced from -2.7±5 μV to -1.1±1.9 μV. Differences between the corrected latencies and amplitudes and the true values were not statistically significant, while differences between uncorrected estimates and true values were statistically significant ($p<0.05$).

Fig. 3 shows a scatter-plot of estimated peak-to-peak amplitudes for this dataset. Tests in which the algorithm misidentified later waveform features as SNAP are clearly seen as they correspond to very low amplitudes. After SA correction, the correlation between estimated and true amplitudes is statistically significant ($r = 0.968$, $p<0.01$).

A second, clinical dataset consisting of 300 nerve conduction studies was also used for testing. Algorithm performance for this dataset was reviewed by neurologists who specialize in electrodiagnostic testing.

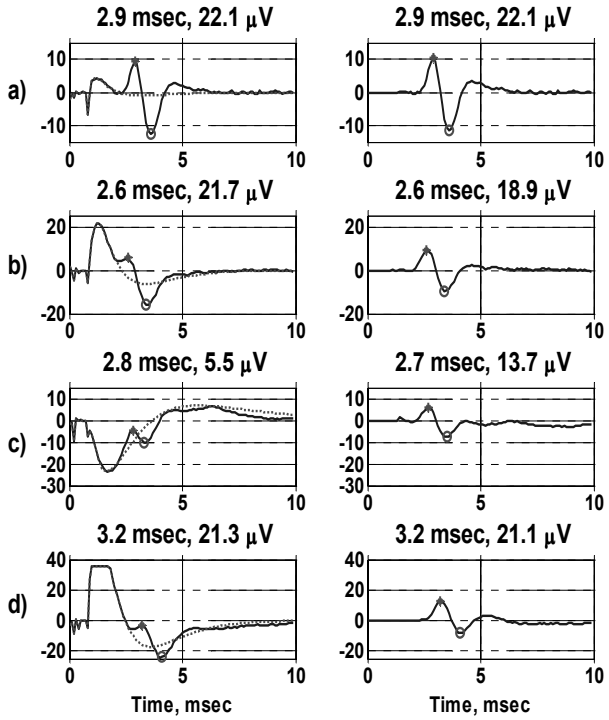

Fig. 4: Examples of stimulus artifact fitting and removal taken from the clinical dataset. Left panel shows uncorrected data (solid) and artifact fit (dotted line) for each test; right panel shows the corrected waveform. SNAP up-peaks ('+') and down-peaks ('o') found by the automated search algorithm are also shown. The latency for the SNAP up-peak and the peak-to-peak amplitude are shown above each waveform.

Example results are shown in Fig. 4. The left subpanels show the uncorrected data and best-fit stimulus artifact model for each test, while the right subpanels show corrected data. The SNAP latency and peak-to-peak amplitude are indicated for each case. Fig. 4a) shows a case in which the SA does not affect the clinically significant parameters. However, removing the SA gives an improved display. In Fig. 4b) the artifact and the SNAP significantly overlap, with the result that SNAP amplitude is overestimated in the uncorrected data. SA removal corrects this discrepancy.

Fig. 4c) shows an example where the artifact deflection is downward. Finally, Fig. 4d) shows an example where the early portion of the SA is clipped.

The clinical dataset was also used to examine the overall impact of SA. A statistical comparison was made of SNAP amplitudes estimated with and without artifact removal. Tests were included in the comparison if: 1) non-negligible SA was seen (defined as SA peak > 2 μV); 2) the SA fit satisfied Eq. 2; 3) automated SNAP parameter estimates were made for both uncorrected and corrected waveforms; 4) the estimated SNAP amplitude exceeded typical noise fluctuations (defined as p2p>2.1 μV); and 5) the estimated latencies (uncorrected and corrected) matched to within 10%, ensuring that the same waveform feature was identified in both cases. Of the 300 tests studied, 67 met these criteria.

Fig. 5 shows a histogram of the amplitude changes caused by SA correction. The most common outcome was an amplitude change of less than 2 μV. For these tests (as in the top panel of Fig. 4) SA removal gave improved data displays. Larger amplitude changes are observed in other tests Results are shown separately for the 50 tests with upward SA deflection and the 17 tests with downward SA deflection. Upward-deflected SA (if uncorrected) leads to an overestimate of SNAP amplitude, while downward SA leads to under-estimation. Artifact removal acts to remove these biases. As seen from Fig. 5, downward-deflected SA was less common in this dataset but caused greater amplitude distortions if uncorrected.

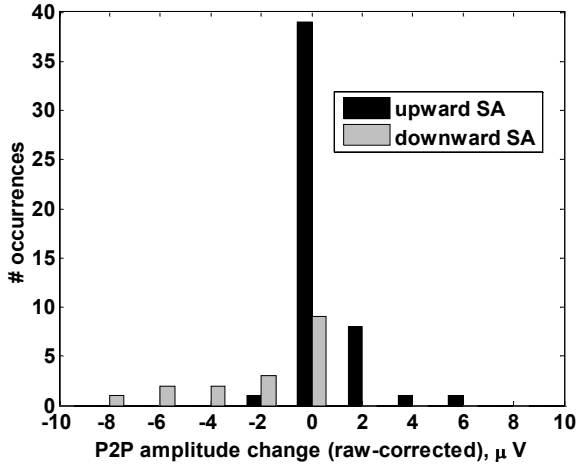

Fig. 5: Histograms showing amplitude changes for positive and negative baseline in the clinical dataset.

V. Summary

A hardware-based model of the stimulus artifact seen in nerve conduction studies was developed and used to estimate and remove the artifact. Based on model parameters that are estimated from the data, the model gives an estimate of the stimulus artifact for all time samples. Thus parameter estimates derived from a small, signal-free portion of the data can be used to correct the measurement during time periods when signal is present. This is important as the stimulus artifact and nerve signal often temporally overlap. Data from sural sensory nerve conduction studies were used to demonstrate that artifact removal can lead to improved estimates of clinically significant parameters.

References

[1] S.N. Gozani, M.A. Fisher, X. Kong, J.T. Megerian, and S.B. Rutkove, "Electrodiagnostic automation: principles and practice," Phy. Med. Rehabil. N. Am., Vol 16, pp. 1015-1032, 2005.

[2] A.I. Vinik, V. Bril, W. J. Litchy, K.L. Price, E.J. Bastyr, and the MBBQ Study Group, "Sural sensory action potential identifies diabetic peripheral neuropathy responders to therapy," Muscle and Nerve, p 619-625, Nov. 2005.

[3] K.C. McGill, K.L. Cummins, L.J. Dorman, B.B. Berlizot, K. Luetkemeyer, D.G. Nishimura, and B. Widrow, "On the nature and elimination of stimulus artifact in nerve signals evoked and recorded using surface electrodes," IEEE Trans. Biomed. Eng., Vol. BME-29, No. 2, pp. 129-137, 1982.

[4] R.N. Scott, L. McLean, and P.A. Parker, "Stimulus artifact in somatosensory evoked potential measurement," Med. Biol. Eng. Comp., Vol. 35, pp. 211-215, 1997.

[5] M.J. Kornfield, J. Cerra, and D.G. Simmons, "Stimulus artifact reduction in nerve conduction," Arch. Phys. Med. Rehab., Vol. 66, pp. 232-235, 1985.

[6] M.B. Wells, "Single channel independent component analysis and its application within an expert system for peripheral neuromuscular data analysis,", Proc. of the 4th International Conf. on Neural Networks and Expert Systems in Healthcare and Medicine, September 2001.

[7] D.A. Wagenaar, and S.M. Potter, "Real-time multi-channel stimulus artifact suppression by local curve fitting," J. Neuro. Methods, Vol. 120, pp. 113-120, 2002.

[8] G.W. Harding, "A method for eliminating the stimulus artifact from digital recordings of the direct cortical response," Comp. Biomed. Res., Vol 24, pp. 183-195, 1991.